

# Theoretical Modeling of the Nuclear-Field Induced Tuning of the Electron Spin Precession for Localized Spins

Nataliia E. Kopteva,\* Irina A. Yugova, Evgeny A. Zhukov, Erik Kirstein, Eiko Evers, Vasili V. Belykh, Vladimir L. Korenev, Dmitri R. Yakovlev, Manfred Bayer, and Alex Greilich

This work is devoted to a theoretical analysis of the effect of nuclear-induced field (Overhauser field) on the Larmor frequencies of electron spins under the periodic pulsed excitation. To describe the dynamical nuclear spin polarization, we use the model where the optically induced Stark field determines the magnitude and direction of the Overhauser field. The Stark field strongly depends on the detuning between the photon energy of excitation and the optical transition energy in the quantum system. Detailed calculations which show that the precession frequencies of fluorine donor-bound electron spins in ZnSe deviate from the linear dependence of the Larmor frequencies on the external magnetic field have been performed. A similar effect is observed for the (In,Ga)As/GaAs quantum dots, where it has been shown that the Overhauser field strongly changes the spectrum of the electron spin precession frequencies.

the electron spin coherence. To suppress nuclear spin fluctuations<sup>[4–6]</sup> one can use the strong feedback mechanism in the electron-nuclear system.<sup>[3,7]</sup> For example, in a transverse-to-beam magnetic field (Voigt geometry) periodic optical pumping of resident electron spins leads to the stabilization of the electron-nuclear system, i.e., it leads to the effect of tuning the frequency of electron spin precession to precession modes that are synchronized with a laser pulse protocol (nuclear-induced frequency focusing effect).<sup>[8]</sup> A few possible mechanisms are suggested to explain the nuclear frequency focusing effect.<sup>[8–13]</sup> The main attention was paid to the study of mechanisms which are based on the electron spin orientation using resonant excitation of corresponding

## 1. Introduction

The relaxation of strongly localized electron spins in semiconductor structures is mainly due to interactions with nuclear spins in the crystal.<sup>[1–3]</sup> These nuclear spins act as a fluctuating local magnetic field, which leads to accelerated dephasing of

optical transitions.


Naturally, at first glance, a resonant optical excitation provides the highest efficiency of electron spin polarization. However, the nonresonant optical excitation of trions is more efficient for the transfer of polarization from electron spins to the system of nuclear spins. This excitation in the Voigt geometry creates the electron spin polarization component along the external magnetic field.<sup>[10]</sup> This component does not oscillate and leads to the efficient flip-flop processes between the electron and nuclear spins. Here we present detailed theoretical modeling of the nuclear frequency focusing effect in the case of nonresonant excitation within the pulse spectrum for the homogeneous and the inhomogeneous spin systems<sup>[10]</sup> in the frames of the dynamical nuclear polarization model. The theoretical results are compared with existing results of pump-probe Kerr rotation experiments on ZnSe epilayer with fluorine doping and on n-doped (In,Ga)As quantum dots.

N. E. Kopteva, Dr. I. A. Yugova  
Physical Faculty of St. Petersburg State University  
198504 St. Petersburg, Russia  
E-mail: st023907@student.spbu.ru

Dr. E. A. Zhukov, E. Kirstein, E. Evers, Dr. V. V. Belykh,  
Prof. D. R. Yakovlev, Prof. M. Bayer, Dr. A. Greilich  
Experimentelle Physik 2  
Technische Universität Dortmund  
44221 Dortmund, Germany

Dr. V. V. Belykh  
P.N. Lebedev Physical Institute of the Russian Academy of Sciences  
119991 Moscow, Russia

Dr. V. L. Korenev, Prof. D. R. Yakovlev, Prof. M. Bayer  
Ioffe Institute  
Russian Academy of Sciences  
194021 St. Petersburg, Russia

 The ORCID identification number(s) for the author(s) of this article can be found under <https://doi.org/10.1002/pssb.201800534>.

DOI: 10.1002/pssb.201800534

## 2. Dynamical Nuclear Polarization via Energy Detuned Excitation

Strong localization of wave functions of resident carriers in quantum structures gives a strong hyperfine interaction between these carriers and nuclei.<sup>[15]</sup> Conduction electrons have s-type of a wave function. An overlapping of this wave function with the

nuclei is provided by Fermi-contact interaction. The Fermi contact interaction is described by an  $\mathbf{I} \cdot \mathbf{S}$  term, which provides the energy for spin flips between electron ( $\mathbf{S}$ ) and nuclear spins ( $\mathbf{I}$ ).<sup>[15]</sup> This term can lead to dynamical nuclear polarization or electron spin dephasing. The dynamical nuclear polarization along the external magnetic field ( $\mathbf{B}||x$ ) in the stationary case can be described by a transcendental equation where the nuclear polarization depends on the electron polarization and vice versa<sup>[10,15,16]</sup>

$$I_N = f_N \bar{Q} \langle S_x(I_N) \rangle. \quad (1)$$

$I_N$  is average nuclear spin,  $f_N = \frac{T_{1L}}{T_{1L} + T_{1e}}$  is the leakage factor,  $T_{1e}$  is the nuclear relaxation time due to interaction with electrons, and  $T_{1L}$  is the nuclear spin-lattice relaxation time, which takes into account any other possible leakage;  $\bar{Q} = 4I(I+1)/3$ ,  $I$  is the nuclear spin. In this model electrons polarized along the external magnetic field polarize nuclear spins along the  $x$ -axis. This nuclear polarization produces a nonzero Overhauser field (OF)  $B_N = \sum_i A_i I_{N,i} \chi_i / \mu_B g$  which acts back on the electrons. Here  $i$  defines the isotope type.  $A$  is the hyperfine constant,  $\chi$  is the nuclear isotope abundance,  $\mu_B$  is the Bohr magneton and  $g$  is the electron  $g$ -factor.

We consider the optical orientation of electron spin polarization excited by circularly polarized pulses along the  $z$ -axis. If laser optical frequency is in resonance with the transition of the negatively charged trion ( $T^-$ ), the electron spin is polarized along  $z$ -axis, and spin precession about the transverse external magnetic field ( $B_x$ ) occurs. Further, if the nonresonant laser pumping of the spin system is applied, one can consider it as an additional effective magnetic field along the  $z$ -axis (the Stark field,  $\omega_s$ ),<sup>[17]</sup> which rotates the spin in the  $xy$  plane and creates a nonzero  $S_x$  component of the electronic polarization. One can write the  $x$ -component of the electron spin polarization after a single pulse action  $S_x^a$  via the spin components before the pulse arrival  $S_{x,y}^b$ <sup>[18]</sup>

$$S_x^a = Q \cos\Phi S_x^b + Q \sin\Phi S_y^b. \quad (2)$$

Here  $Q$  and  $\Phi$  are pulse amplitude and phase, respectively. They depend on the pulse area ( $\theta$ ) and the optical detuning ( $\Delta$ ).<sup>[18]</sup> For estimations, a spectrally smooth Rosen-Zener pulse is used<sup>[19]</sup>

$$f(t) = \frac{\mu}{\cosh(\pi t / \tau_p)}. \quad (3)$$

The coefficient  $\mu$  is the measure of the electric field strength and  $\tau_p$  is the pulse duration. Rosen-Zener pulse amplitude  $Q$  and phase  $\Phi$  are defined by

$$Q = \left| \frac{\Gamma^2(\frac{1}{2} - i\Delta)}{\Gamma(\frac{1}{2} - i\Delta - \frac{\theta}{2\pi})\Gamma(\frac{1}{2} - i\Delta + \frac{\theta}{2\pi})} \right|, \quad (4)$$

$$\Phi = \arg \left( \frac{\Gamma^2(\frac{1}{2} - i\Delta)}{\Gamma(\frac{1}{2} - i\Delta - \frac{\theta}{2\pi})\Gamma(\frac{1}{2} - i\Delta + \frac{\theta}{2\pi})} \right), \quad (5)$$

here  $\theta = \mu\tau_p$  is the pulse area.  $\Delta = (E_p - E)\tau_p / 2\pi\hbar \equiv \Delta E\tau_p / 2\pi\hbar$  is proportional to the energy gap ( $\Delta E$ ) between the pump photon

energy ( $E_p$ ) and the transition energy ( $E$ ). One should note that at resonant optical excitation  $\Phi = 0$  and therefore an  $S_x$  component is not created by the pulse.

In case of excitation by an infinitely long sequence of circularly polarized pulses, the averaged (over the laser repetition time)  $S_x$  component of the electronic polarization is given by<sup>[18]</sup>

$$\langle S_x(t) \rangle = \frac{T_2}{T_R} \left( 1 - e^{-T_R/T_2} \right) \times \frac{K(1 - Q^2)\sin(\omega T_R)}{4(1 + LM - (L + M)\cos(\omega T_R))}. \quad (6)$$

Here

$$K = \frac{Qe^{-T_R/T_2}\sin\Phi}{1 - Qe^{-T_R/T_2}\cos\Phi}, \quad (7)$$

$$M = Q(\cos\Phi - K \sin\Phi) \cdot e^{-\frac{T_R}{T_2}}, \quad (8)$$

$$L = \frac{1 + Q^2}{2} \cdot e^{-\frac{T_R}{T_2}}. \quad (9)$$

Here  $T_2$  is the homogeneous electron spin relaxation time in a transverse external magnetic field,  $T_R$  is the repetition period of the laser,  $\omega = \omega_x + \omega_N \equiv \mu_B g(B_x + B_N) / \hbar$  is the electron precession frequency in the total magnetic field and  $\hbar$  is the reduced Planck constant.

The  $\langle S_x \rangle$  dependence on the external magnetic field ( $B_x$ ) is shown in **Figure 1(a)**. One can see that this dependence has a dispersive form around  $\omega_x / \Omega_R = N$  ( $N$  is an integer number), but inverted signs for different detunings.<sup>[20]</sup> The OF obtained from Equation (1), (6)–(9) shows different behavior in dependence on  $\omega_x$  for different detunings (Figure 1(b)). For negative detunings, it has a maximal magnitude near the condition  $\omega_x / \Omega_R = N$ . For positive detunings, the maximal magnitude of the OF is close to  $\omega_x / \Omega_R = N + 1/2$ . This can be explained as follows. In the case of a coordinate system rotating with  $N\Omega_R$ , electron spin precesses in an effective magnetic field with the frequency  $\omega_x - N\Omega_R$  (Figure 1(c) and (d)). At the resonance, where  $\omega_x = N\Omega_R$  the electron spin  $S$  is maximal and is equal to  $S_0$ . In this case, no nuclear polarization is created and  $\omega_N = 0$ . Additionally, the electron spin is affected by the optically induced Stark field, which is directed along  $Z'$ . The sign of optical detuning  $\Delta$  from the optical transition resonance defines the direction of the effective field relative to the spin: if detuning  $\Delta > 0$ ,  $\omega_s$  is antiparallel to  $S_0$ , see Figure 1(c). If  $\Delta < 0$ , these are parallel, Figure 1(d). These directions depend on the  $g$ -factor sign and are given here for a positive  $g$ -factor, as in the case of fluorine-doped ZnSe.

If the  $\omega_x$  shifts away from the  $N\Omega_R$ , a tilted field  $\omega$  appears which leads to a non-zero electron spin projection in the  $x$ -direction,  $S_x$ . It allows a buildup of nuclear field  $\omega_N$  as a result of a flip-flop processes between the constant electron spin and nuclear system. For the  $\Delta > 0$  the nuclear field is directed in the opposite direction to the external field. It creates feedback that

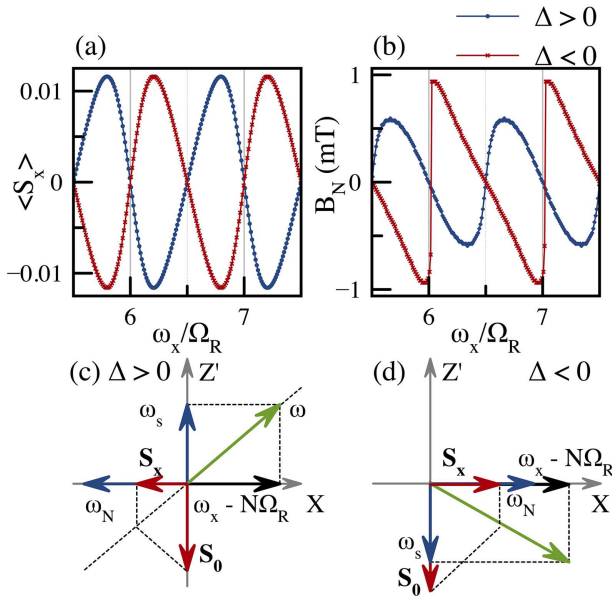


**Figure 1.**  $\langle S_x \rangle$  (a) and the Overhauser field (b) dependencies on the external magnetic field for positive (blue line) and negative (red line) detunings. Calculation parameters:  $\theta = \pi$ ,  $T_2 = 1.5T_R$ ,  $\Omega_R = 2\pi/T_R$ ,  $\Delta E = \pm 0.16$  meV,  $g = 1.13$ .  $^{77}\text{Se}$  isotope parameters are used (see Table 1). Vector diagrams for fields affecting the electron-nuclear spin system in the rotating frame for positive (c) and negative (d) detunings.

locks the Larmor frequency of electron near  $N\Omega_R$ , as the smallest shifts away from the mode frequency, are compensated by oppositely directed nuclear field.

The situation inverts in case of the optical detuning  $\Delta < 0$ . In this case, the Stark field direction is changed. The nuclear field is directed in the same direction as the external field, which drives the electron precession away from the mode  $N\Omega_R$ . In this case, the modes are non-stable, and the stability is given in between the modes. Finally, the difference in the form of the curves in Figure 1(b) can be related to the difference of the feedback conditions. The OF is added to (or subtracted from) the external magnetic field and non-resonant optical pumping will deviate the electronic precession frequency from the Larmor frequency in the external magnetic field.<sup>[10,20,21]</sup> Note that the sign of the g-factor determines the relation between the detuning sign and the synchronization condition.

Equations (2)–(9) are written for a single spin system or a homogeneous spin ensemble with equal g-factors and optical detunings. If  $\bar{Q}f_N\delta S_x(I_N)/\delta I_N < 1$  then Equation (1) has one solution and  $B_N < B_0$  ( $B_0 \equiv \hbar\Omega_R/2g\mu_B$ ). The back action of the nuclear polarization on a single electronic spin (homogeneous spin ensemble) tunes and fixes the electronic precession frequencies in the transverse external magnetic field to the condition  $\omega_x/\Omega_R = N$  (phase synchronization condition) for positive detunings and to  $\omega_x/\Omega_R = N + 1/2$  for negative detunings. Herewith additional precession frequencies do not appear for a single spin (homogeneous spin ensemble) in the spin precession spectrum.<sup>[22]</sup>

If  $\bar{Q}f_N\delta S_x(I_N)/\delta I_N > 1$  then Equation (1) has a set of solutions and  $B_N > B_0$ . Therefore two (or more) possibilities for electron

precession frequency tuning exist for each value of the external magnetic field. It gives multiple spin precession modes in the spectrum. This is an analog of an inhomogeneous spin system due to the appearance of several precession frequencies in an initially homogeneous ensemble.

In an inhomogeneous spin ensemble with a nonzero spread of g-factors ( $\delta g$ ) a small OF can provide a multiple modes regime, if  $\mu_B\delta g B_x/\hbar > \Omega_R$ . If the g-factor linearly depends on the energy of the optical excitation ( $E_p$ ),<sup>[18]</sup> we expect the appearance of two ensembles in the spectrum of the electron precession frequencies. For the negatively detuned ensemble the OF tunes the Larmor frequencies into  $\omega_x/\Omega_R = N$ . For the positively detuned ensemble the OF tunes the Larmor frequencies into  $\omega_x/\Omega_R = N + 1/2$ . Moreover, a large OF can overlap several modes of synchronization. Thus the electronic spectrum becomes broader and additional modes of precession appear.

### 3. Estimations of the Maximal Overhauser Field for the Different Types of the Nuclei

We consider now two systems and compare them with the experimental data. The first one is a homogeneous spin system based on a ZnSe epilayer doped with fluorine donors. In this system, resident electrons are bound on the donors which results in a strong localization of electrons.<sup>[23]</sup> Due to localization a long electron spin coherence time in a transverse magnetic field is present in the systems. Further, we use ratio  $T_2/T_R = 5$ <sup>[24]</sup> for the theoretical estimations. The second system is an inhomogeneous one, which is realized in an (In,Ga)As quantum dot (QD) ensemble. In this system, resident electrons are strongly localized by the quantum dot potential and have an even longer spin coherence time, modeled by  $T_2/T_R = 80$ .<sup>[25]</sup> The nuclear parameters for both structures are collected in Table 1. We make estimations for the maximal Overhauser fields achievable in these systems for different ratios  $T_2/T_R$ . The OF is limited by the maximal value of  $\langle S_x \rangle$ . From Equation (6) we obtain

$$\langle S_x \rangle_{\max} = \frac{T_2 (1 - \exp(-T_R/T_2))K(1 - Q^2)}{4\sqrt{(1 - M^2)(1 - L^2)}}. \quad (10)$$

The  $\langle S_x \rangle$  dependence on the pulse area and the ratio  $T_2/T_R$  are presented in Figure 2(a) and (b), respectively. One can see that  $\langle S_x \rangle_{\max}$  has a maximal magnitude for  $\theta = \pi$  (Figure 2(a)) where  $\langle S_x \rangle$  saturates for  $T_2/T_R > 20$ .

**Table 1.** Constants for different types of nuclei. Data for nuclear spin and abundance is taken from ref. [27]. Data for hyperfine constants (for all isotopes except  $^{115}\text{In}$ ) is taken from ref. [28] and references therein. The hyperfine constants of  $^{115}\text{In}$  is taken from ref. [29].

	$^{77}\text{Se}$	$^{67}\text{Zn}$	$^{75}\text{As}$	$^{71}\text{Ga}$	$^{69}\text{Ga}$	$^{115}\text{In}$
A, $\mu\text{eV}$	33.6	3.7	46	48.5	38.2	56
x, %	7.58	4.11	100	39.8	60.2	95.77
I	1/2	5/2	3/2	3/2	3/2	9/2

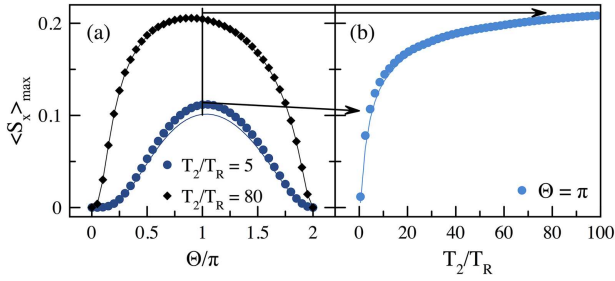


**Figure 2.** The  $\langle S_x \rangle$  dependence on (a) pulse area for  $T_2/T_R = 5$  and  $80$  and on (b) ratio  $T_2/T_R$  for  $\theta = \pi$ .

Not only  $\langle S_x \rangle_{\max}$  limits the maximal OF. One can see from Equation (11) that also the nuclear isotope abundance ( $\chi$ ), the electronic g-factor and the leakage factor ( $f_N$ ) limit  $B_N$

$$B_{N,\max} = \frac{A f_N \chi \bar{Q}}{\mu_{BG}} f_N \langle S_x \rangle_{\max}. \quad (11)$$

For fully polarized nuclei the OF is described by the equation  $\bar{B}_N = A \chi / \mu_{BG}$ .<sup>[26]</sup> For simplicity, we normalize Equation (11) on  $\bar{B}_N$ , so that we obtain

$$\frac{B_{N,\max}}{\bar{B}_N} = f_N \bar{Q} \langle S_x \rangle_{\max}. \quad (12)$$

The results of the maximal OF calculations are presented in Table 2. We assume  $T_{1L} \gg T_{1e}$  and  $f_N = 1$  for the ZnSe structure.<sup>[30]</sup> One can see for ZnSe based structure that  $B_{N,\max}$  is much stronger for selenium nuclei, then for zinc nuclei due to the difference in hyperfine constants. The magnitude of  $B_{N,\max}$  for selenide nuclei exceeds  $B_0 = 2.4$  mT (for  $T_R = 13.2$  ns), which leads to the possibility to cover the full range between the modes. The dependences of the OF on the external magnetic field for positive and negative detunings  $\pm 0.16$  meV are shown in Figure 3(a) and (b). One can see that for  $\Delta E = \pm 0.16$  meV the OF does not reach maximal values. However in the same region of external magnetic fields two different values of  $B_N$  are present simultaneously and a hysteresis regime appears. As presented in Figure 3(c) and (d) nuclear feedback on the electrons fixes the precession frequency of the electron spin in the external and OF to two modes simultaneously. It gives rise to observations of a multiple modes regime in this structure.<sup>[10]</sup>

**Table 2.** The maximal Overhauser field for different types of nuclei for  $f_N = 1$ ,  $\theta = \pi$ ,  $T_2/T_R = 5$  and  $80$ .

	<sup>77</sup> Se	<sup>67</sup> Zn	<sup>75</sup> As	<sup>71</sup> Ga	<sup>69</sup> Ga	<sup>115</sup> In
$T_2/T_R = 5$						
$B_{N,\max}$ , T	0.004	0.001	0.8	0.32	0.4	6
$\frac{B_{N,\max}}{\bar{B}_N}$ , %	10	46	50	50	50	100
$T_2/T_R = 80$						
$B_{N,\max}$ , T	0.008	0.002	1.6	0.65	0.8	12
$\frac{B_{N,\max}}{\bar{B}_N}$ , %	20	92	100	100	100	100

For estimations of  $B_{N,\max}$  in (In,Ga)As quantum dots we also assume  $T_{1L} \gg T_{1e}$  and  $f_N = 1$ . Due to the strong hyperfine interaction and high isotope abundance  $B_{N,\max}$  reaches  $\approx 1$  T for these structures (see Table 2).<sup>[26]</sup> The maximal OF corresponds to indium nuclei. However, these calculations do not take into account the concentration of indium in the QD nor the fact that  $f_N \neq 1$  in real systems. The magnitude of  $B_{N,\max}$  for all types of nuclei exceeds  $B_0 = 6$  mT and the OF overlaps several precession modes in the QD ensemble. Thus the electronic spectrum becomes broader and additional modes of precession appear due to the nuclear feedback effect. For rough estimations of the number of additional modes in case of  $B_N < B_x$  Equation (6) can be written near modes ( $\omega_x = N\Omega_R$ ,  $N$  is an integer) as

$$\langle S_x \rangle = \frac{S_0 \omega_N}{(1 + LM) - (L + M) + 0.5(L + M)(\omega_N T_R)^2}, \quad (13)$$

$$S_0 = T_2 K (1 - Q^2) (1 - e^{-T_R/T_2}) / 4. \quad (14)$$

It is convenient to represent the OF using Equation (1) as

$$(\omega_N T_R)^2 = 2 \left[ -\frac{(L-1)(M-1)}{L+M} + \frac{A \chi \bar{Q}}{\hbar} \frac{S_0}{L+M} \right]. \quad (15)$$

The number of electron spin precession modes overlapped by the OF is shown in Figure 4 for different pump powers as a function of the detuning. One can see that the OF shows a strong asymmetry on the detunings. Moreover, an increase of the pump power leads to an increase of the OF and precession modes number in the QD ensemble. For these estimations, we have reduced the leakage factor in order to achieve the regime where  $B_N < B_x$ .

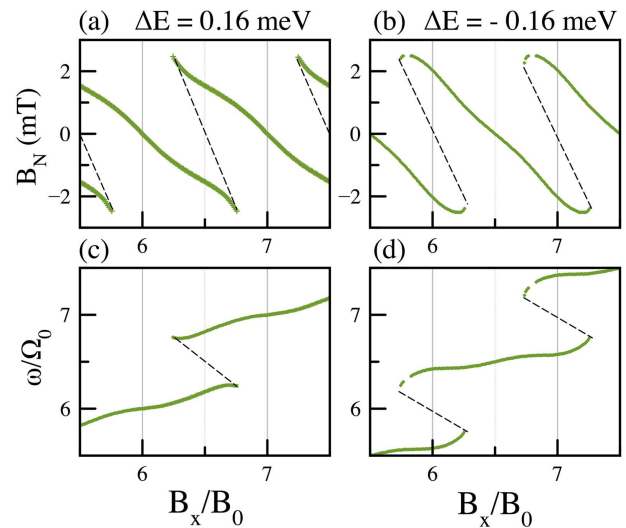


**Figure 3.** The Overhauser field dependences on the external magnetic field for positive (a) and negative (b) detunings. The electron spin precession frequency dependence for positive (c) and negative (d) detunings. Calculation parameters:  $\theta = \pi$ ,  $T_2 = 5T_R$ ,  $\Delta E = \pm 0.16$  meV,  $g = 1.13$ . <sup>77</sup>Se isotope parameters are used (see Table 1).



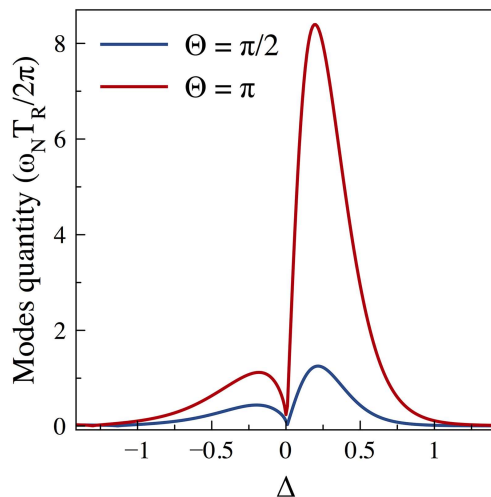


**Figure 4.** The Overhauser field dependencies on the detuning for different pulse areas. Parameters:  $T_2 = 7T_R$ ,  $f_N = 0.1$ ,  $^{71}\text{Ga}$  nuclei (see parameters in Table 1).

#### 4. Experimental Evidence

As mentioned above, the electron spin is initialized by pulsed optical pumping that induces dynamical nuclear polarization. The back action of the dynamical nuclear polarization on the electronic spins changes the precession frequency in the external magnetic field. The observation of this effect is possible in the pump-probe time-resolved Kerr rotation experiments<sup>[14]</sup> in systems with strong electron localization in a transverse external magnetic field. Circularly polarized pump pulses create a non-zero electron spin polarization which precesses about the external magnetic field and decreases due to spin relaxation processes. This polarization and its precession are detected by the rotation angle of the linearly polarized probe pulse reflected from the polarized medium of the sample. Pump and probe pulses are delayed relative to each other by a mechanical delay line to allow us to study the time dynamics of Kerr rotation amplitude by variation of the delay. Laser repetition period  $T_R$  limits the spin coherence time measured by this method. More advanced configuration of this technique called extended pump-probe<sup>[31]</sup> allows measuring full spin dynamics in case of spin relaxation  $T_2 > T_R$ . In that configuration, the pump laser is modulated by the intensity with an electro-optical modulator, which controls the number of pump-pulses separated by  $T_R$  in a pump-train sent to the system for initialization of the spin polarization. The probe laser is modulated by an acousto-optic modulator, which picks a single probe pulse that is delayed electronically in units of  $T_R$  from the pump-train. A mechanical delay line can also provide fine delay scans within the  $T_R$ . It allows one to extend the time windows between separate excitations by several orders of magnitude and to observe the free spin dynamics between the pump-pulse-trains with picosecond resolution. The Fourier transform of free spin dynamic gives the spectrum of spin precession modes in the ensemble of QDs.

The experimental results for the ZnSe sample are obtained by the classical time-resolved pump-probe technique. In **Figure 5**, the experimental and theoretical dependencies of

the electron spin precession frequency on the external magnetic field is shown for different pump powers.<sup>[32]</sup> One can see that the frequency dependence on the external magnetic field is step-like. In the case of low power, the frequency is fixed at the value  $B_x/B_0 = N$  (the phase synchronization conditions). Increasing the pump intensity leads to a frequency locking at  $B_x/B_0 = N + 1/2$ . At positive detunings (Figure 5(b)), the OF shifts the electron precession frequency toward the phase synchronization conditions. For negative detunings, the nuclear polarization pulls the precession frequency away from the whole integer of the modes for the phase synchronization conditions. This effect allows one to tune the electron spin precession frequencies to or away from the modes of the phase synchronization conditions.

A similar effect is observed in extended pump-probe experiments for the (In,Ga)As/GaAs quantum dots with a large inhomogeneous broadening of electron g-factors.<sup>[33]</sup> In **Figure 6(a)** the experimental precession frequency spectrum for the inhomogeneous QD ensemble is shown. The peaks in this distribution correspond to the density of states in the ensemble of QDs. One can see in Figure 6(a) that the peaks are fixed at whole integers of the mode positions corresponding to the phase synchronization condition for oscillators with smaller frequency. However, for larger frequencies, the peaks are between the modes. Theoretical spectra for the negatively and the positively detuned ensemble of electrons are shown in Figure 6(b). Positive (negative) optical detunings give an adjustment to half-integer modes (integer modes). Here we assume that the

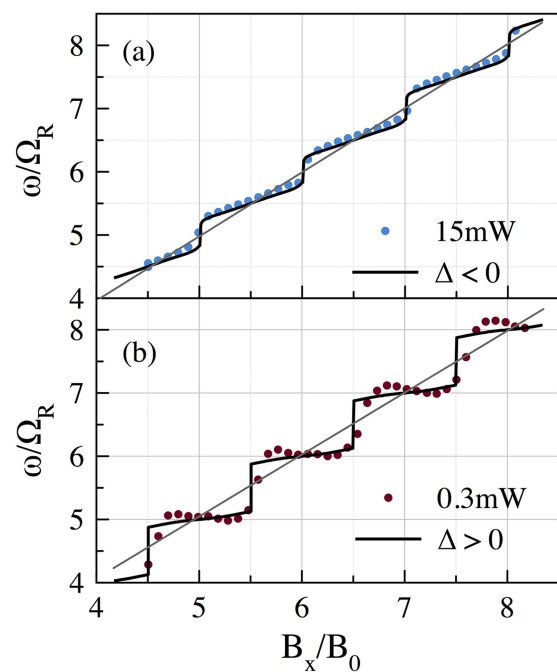


**Figure 5.** Dots (experimental results for ZnSe epilayer<sup>[32]</sup>): the frequency dependence on the external magnetic field for high power excitation (a) and low power excitation (b). Lines show the results of calculations: for negative detuning (a) and for positive detuning (b). Grey line corresponds to zero OF.

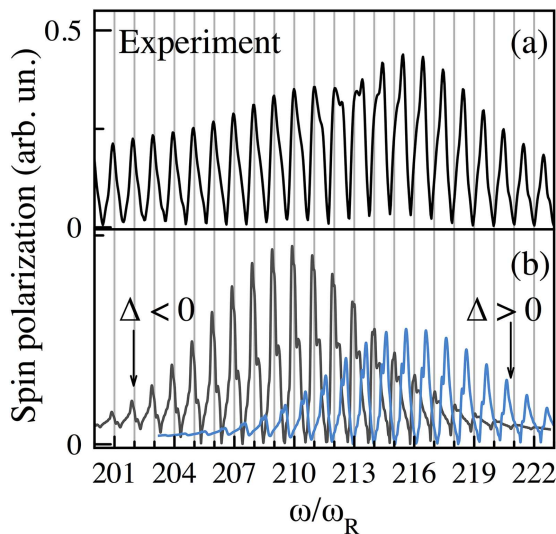


**Figure 6.** a) Experimental spectrum of the spin polarization in an ensemble of QDs at  $B_x = 2$  T and  $T = 5$  K.<sup>[33]</sup> b) Calculated spectrum of the spin polarization. A linear g-factor dependence on the detuning is assumed. Parameters:  $T_2 = 45T_R$ ,  $\theta = \pi$ ,  $B_x = 2T$ ,  $f_N = 0.05$  calculated for  $^{71}\text{Ga}$  nuclei (see parameters in Table 1). For the blue line  $\Delta E = 0.27$  meV, for the gray line  $\Delta E = -0.29$  meV.

g-factor is negative and its average value depends linearly on the energy of the optical excitation. Due to the opposite g-factor sign, the detuning sign for the InGaAs QDs is opposite to the one for the ZnSe epilayer.

## 5. Conclusion

The nuclear frequency focusing effect leads to a discretization of the electron spin precession frequencies. The conditions of this discretization depend on the optical detuning between the pump energy and the electron transition. The strong feedback in the electron-nuclear spin system allows one to tune the electron spin precession frequencies so that they are adjusted to the integer or half-integer numbers of the laser pulse repetition frequency.

We estimate the maximal Overhauser field for different types of nuclei in the dynamical nuclear polarization model and find that the appearance of additional precession modes or the hysteresis behavior in precession frequencies depends on the strength of the interaction between the electron spin and the nuclear spins. This is related to the Overhauser nuclear field, which can overlap several precession modes.

For a homogeneous ensemble in case of  $B_N < B_0$  the discretization leads to the formation of plateaus in the dependence of the precession frequency on the external magnetic field (single-mode regime).

For an inhomogeneous ensemble of localized spins, the broadening of the precession spectrum and the appearance of additional half-integer modes can lead to strong changes in the amplitude of the spin mode locking signal<sup>[34]</sup> and to the complex dependence of its amplitude on the laser pulse protocol and the external magnetic field.<sup>[35,36]</sup>

## Acknowledgments

This work was supported by Deutsche Forschungsgemeinschaft and the Russian Foundation of Basic Research (Grant No. 19-52-12059) in the frame of ICRC TRR 160 (Project A1). N.E.K. and I.A.Y. acknowledge support from Saint Petersburg State University (Grant No. 11.34.2.2012 ID 28874264). V.V.B. acknowledges support from the Russian Science Foundation (Contract No. 18-72-10073).

## Conflict of Interest

The authors declare no conflict of interest.

## Keywords

electron–nuclei spin interactions, Overhauser field, spin coherence

Received: September 29, 2018

Revised: December 12, 2018

Published online:

- [1] *Spin Physics in Semiconductors* (Ed: M. I. Dyakonov), Springer-Verlag, Berlin **2008**.
- [2] *Optical Orientation* (Eds: F. Meier, B. P. Zakharchenya), North-Holland, Amsterdam **1984**.
- [3] M. M. Glazov, *Electron and Nuclear Spin Dynamics In semiconductor Nanostructures*, Oxford University Press, Oxford **2018**.
- [4] I. A. Merkulov, Al. L. Efros, M. Rosen, *Phys. Rev. B* **2002**, *65*, 205309.
- [5] A. V. Khaetskii, D. Loss, L. Glazman, *Phys. Rev. Lett.* **2002**, *88*, 186802.
- [6] A. Khaetskii, D. Loss, L. Glazman, *Phys. Rev. B* **2003**, *67*, 195329.
- [7] B. Urbaszek, X. Marie, T. Amand, O. Krebs, P. Voisin, P. Maletinsky, A. Högele, A. Imamoğlu, *Rev. Mod. Phys.* **2013**, *85*, 79133.
- [8] A. Greilich, A. Shabaev, D. R. Yakovlev, Al. L. Efros, I. A. Yugova, D. Reuter, A. D. Wieck, M. Bayer, *Science* **2007**, *317*, 5846.
- [9] M. M. Glazov, I. A. Yugova, Al. L. Efros, *Phys. Rev. B* **2012**, *85*, 041303.
- [10] V. L. Korenev, *Phys. Rev. B* **2011**, *83*, 235429.
- [11] M. Y. Petrov, G. G. Kozlov, I. V. Ignatiev, R. V. Cherbunin, D. R. Yakovlev, M. Bayer, *Phys. Rev. B* **2009**, *80*, 125318.
- [12] J. Danon, Y. V. Nazarov, *Phys. Rev. Lett.* **2008**, *100*, 056603.
- [13] E. Barnes, S. E. Economou, *Phys. Rev. Lett.* **2011**, *107*, 047601.
- [14] *Semiconductor Spintronics and Quantum Computation* (Eds: D. D. Awschalom, D. Loss, N. Samarth), Springer-Verlag, Berlin **2002**.
- [15] *The Principle of Nuclear Magnetism* (Ed: A. Abragam), Oxford University Press, Oxford **1961**.
- [16] M. I. Dyakonov, V. I. Perel, *Z. Eksp. Teor. Fiz.* **1973**, *65*, 362.
- [17] C. Cohen-Tannoudji, J. Dupont-Roc, *Phys. Rev. A* **1972**, *5*, 968984.
- [18] I. A. Yugova, M. M. Glazov, E. L. Ivchenko, Al. L. Efros, *Phys. Rev. B* **2009**, *80*, 104436.
- [19] N. Rosen, C. Zener, *Phys. Rev.* **1932**, *40*, 502507.
- [20] S. G. Carter, A. Shabaev, S. E. Economou, T. A. Kennedy, A. S. Bracker, T. L. Reinecke, *Phys. Rev. Lett.* **2009**, *102*, 167403.
- [21] S. G. Carter, S. E. Economou, A. Shabaev, A. S. Bracker, *Phys. Rev. B* **2011**, *83*, 115325.
- [22] A. Greilich, S. Spatzek, I. A. Yugova, I. A. Akimov, D. R. Yakovlev, Al. L. Efros, D. Reuter, A. D. Wieck, M. Bayer, *Phys. Rev. B* **2009**, *79*, 201305.
- [23] A. Pawlis, T. Berstermann, C. Brüggenmann, M. Bombeck, D. Dunker, D. R. Yakovlev, N. A. Gippius, K. Lischka, M. Bayer, *Phys. Rev. B* **2011**, *83*, 115302.

- [24] A. Greilich, A. Pawlis, F. Liu, O. A. Yugov, D. R. Yakovlev, K. Lischka, Y. Yamamoto, M. Bayer, *Phys. Rev. B* **2012**, *85*, 121303.
- [25] A. Greilich, D. R. Yakovlev, M. Bayer, *Solid State Commun.* **2009**, *149*, 1466.
- [26] D. Paget, G. Lampel, B. Sapoval, V. I. Safarov, *Phys. Rev. B* **1977**, *15*, 57805796.
- [27] *American Institute of Physics Handbook*, 3rd ed. (Ed: D. E. Gray), McGraw-Hill, New York **1972**.
- [28] E. A. Zhukov, A. Greilich, D. R. Yakovlev, K. V. Kavokin, I. A. Yugova, O. A. Yugov, D. Suter, G. Karczewski, T. Wojtowicz, J. Kossut, V. V. Petrov, Y. K. Dolgikh, A. Pawlis, M. Bayer, *Phys. Rev. B* **2014**, *90*, 085311.
- [29] M. Y. Petrov, I. V. Ignatiev, S. V. Poltavtsev, A. Greilich, A. Bauschulte, D. R. Yakovlev, M. Bayer, *Phys. Rev. B* **2008**, *78*, 045315.
- [30] F. Heisterkamp, E. Kirstein, A. Greilich, E. A. Zhukov, T. Kazimierczuk, D. R. Yakovlev, A. Pawlis, M. Bayer, *Phys. Rev. B* **2016**, *93*, 081409.
- [31] V. V. Belykh, E. Evers, D. R. Yakovlev, F. Fobbe, A. Greilich, M. Bayer, *Phys. Rev. B* **2016**, *94*, 241202.
- [32] E. A. Zhukov, E. Kirstein, N. E. Kopteva, F. Heisterkamp, I. A. Yugova, V. L. Korenev, D. R. Yakovlev, A. Pawlis, M. Bayer, A. Greilich, *Nat. Commun.* **2018**, *9*, 1941.
- [33] E. Evers, V. V. Belykh, N. E. Kopteva, I. A. Yugova, A. Greilich, D. R. Yakovlev, D. Reuter, A. D. Wieck, M. Bayer, *Phys. Rev. B* **2018**, *98*, 075309.
- [34] A. Greilich, D. R. Yakovlev, A. Shabaev, Al. L. Efros, I. A. Yugova, R. Oulton, V. Stavarache, D. Reuter, A. Wieck, M. Bayer, *Science* **2006**, *313*, 5785.
- [35] N. Jäschke, A. Fischer, E. Evers, V. V. Belykh, A. Greilich, M. Bayer, F. B. Anders, *Phys. Rev. B* **2017**, *96*, 205419.
- [36] I. Kleinjohann, E. Evers, P. Schering, A. Greilich, G. S. Uhrig, M. Bayer, F. B. Anders, *Phys. Rev. B* **2018**, *98*, 155318.